NANO LETTERS

2007
Vol. 7, No. 9
2806−2811

# Scalable Fabrication of Carbon Nanotube/Polymer Nanocomposite Membranes for High Flux Gas Transport

**Sangil Kim,[†] Joerg R. Jinschek,[‡] Haibin Chen,[§] David S. Sholl,[§] and Eva Marand*,[†]**

*Chemical Engineering Department, Virginia Polytechnic Institute and State University, Blacksburg, Virginia 24061-0211, Material Science and Engineering Department, Virginia Polytechnic Institute and State University, Blacksburg, Virginia 24061-0211, and Department of Chemical Engineering, Carnegie Mellon University, Pittsburgh, Pennsylvania 15213*

*Received June 13, 2007; Revised Manuscript Received July 23, 2007*

**ABSTRACT**

**We present a simple, fast, and practical route to vertically align carbon nanotubes on a porous support using a combination of self-assembly and filtration methods. The advantage of this approach is that it can be easily scaled up to large surface areas, allowing the fabrication of membranes for practical gas separation applications. The gas transport properties of thus constructed nanotube/polymer nanocomposite membranes are analogous to those of carbon nanotube membranes grown by chemical vapor deposition. This paper shows the first data for transport of gas mixtures through carbon nanotube membranes. The permeation of gas mixtures through the membranes exhibits different properties than those observed using single-gas experiments, confirming that non-Knudsen transport occurs.**

Carbon nanotubes (CNT) have been identified as fundamentally new nanoporous materials that show great potential for sensors,[1,2] composites,[3] catalytic supports,[4] and as membrane materials.[5,6] In particular, CNTs, whose inner core diameter can be as low as 4 Å,[7,8] have been earmarked as possible selective nanopores in membrane materials.[9,10] Atomistic simulations have predicted that if used as membranes, CNTs should have unprecedented flux and selectivity properties compared to other known inorganic materials. The transport of gases in carbon nanotubes with diameter ∼1 nm was predicted to be orders of magnitude faster than in zeolites.[9−13] These exceptionally high transport rates have been attributed to the inherent molecular smoothness of the nanotubes. Some of these theoretical predictions have been verified experimentally with larger carbon nanotubes.[5,6] Holt et al.[6] have constructed nanotube−$Si_3N_4$ composite membranes using chemical vapor deposition. They used aligned double-walled carbon nanotubes (DWNT) having a diameter of about 1.6 nm and showed that gas flow through the carbon nanotubes is 1−2 orders of magnitude faster than would be expected for flow through a commercial polycarbonate nanoporous membrane with 15 nm pore size. They also found that liquid water flow through their nanotube membranes was more than 3 orders of magnitude faster than expected from hydrodynamic flow calculations. Moreover, these nanotube membranes exhibited extraordinarily high size exclusion selectivity. In related work, Hinds and co-workers[5] constructed polymer−nanotube composite membranes using multiwalled carbon nanotubes (MWNT) having large diameters (6−7 nm). They have verified that transport of liquids (alkanes, water) is orders of magnitude faster than can be accounted for by conventional hydrodynamic flow.[14]

The use of single-walled (SWNT), smaller diameter carbon nanotubes as membranes is particularly intriguing because, in addition to fast transport rates, the 4−12 Å pore openings are in the range that may be size-selective for gas mixtures. For SWNTs to effectively act as channels in a membrane, however, they have to be aligned vertically relative to the penetrant stream. This is perhaps the single most important challenge facing the fabrication of SWNT membranes. In their studies, Hinds et al. and Holt et al. used chemical vapor deposition to grow oriented carbon nanotubes.[5,6] While producing well-aligned carbon nanotubes, this process is expensive, tedious, and is limited to fabricating samples with small areas (e.g., sub-$cm^2$). Alternatively, CNTs have been

* Corresponding author. E-mail: emarand@vt.edu. Telephone: (540)-231-8231. Fax: (540)-321-5022.
[†] Chemical Engineering Department, Virginia Polytechnic Institute and State University.
[‡] Material Science and Engineering Department, Virginia Polytechnic Institute and State University.
[§] Department of Chemical Engineering, Carnegie Mellon University.

10.1021/nl071414u CCC: $37.00 
**Published on Web 08/09/2007**

aligned by employing filtration methods,[15,16] although to date this approach has been successful only with MWNTs.

In this paper, we report on the transport properties of SWNT/polymer nanocomposite membranes fabricated by orienting functionalized SWNTs with a filtration method. We believe that the alignment of the SWNT results from a self-assembly mechanism directed by the shear forces of the flowing solvent stream in combination with repulsive forces between the carbon nanotubes and the nearby membrane filter surface. It has been reported that shear forces align SWNTs in the flow direction.[17] In our samples, SWNTs orient in shear flow and propagate the perpendicular alignment to the filter substrate via long-range repulsive forces that exist between zwitterions attached to the carbon nanotube surface. This phenomena is similar to the orientation behavior of rigid rodlike polyelectrolytes near charged surfaces.[18]

Arc discharge SWNTs were treated using a mixture of $H_2SO_4/HNO_3$ to cut the nanotubes into small lengths and open end tips.[19] The average pore diameter of the SWNT estimated from porosimetry measurements is 1.2 nm. The pore-size distribution is shown in Figure 1a. It has been reported that acids can be intercalated into SWNT bundles and disintegrate the tube walls into graphitic flakes and then reform them into MWNTs.[20] After acid treatment, the prepared CNTs samples are mostly composed of multiwalled carbon nanotubes or transformed SWNTs created during the oxidation, shown in Figure 1b, and bundled SWNTs, shown in Figure 1c. The transformed SWNTs have pore diameters of less than 2 nm and are surrounded by multilayered graphitic shells and amorphous-like carbon materials (Figure 1b). CNT nanocomposite membranes are prepared by dispersing amine-functionalized carbon nanotubes in THF and filtering this solution through a PTFE filter. The oriented carbon nanotubes remaining on the filter are coated with a thin polysulfone (PSF) layer. Polysulfone was chosen as the matrix to impart the membrane with mechanical strength and to seal the structure. The schematic of this process along with an image of the membrane film are shown in Figure 2a. Figure 2b shows the scanning electron microcopy (SEM) images of the CNTs on top of a PTFE membrane filter. Most of the nanotubes are "standing up", although some are not fully aligned vertically to the membrane filter. An SEM image of the composite film in Figure 2c shows that spin-coating the polymer from a dilute solution allows the polymer to penetrate well around the nanotubes and allows most nanotube tips to be slightly exposed above the polymer matrix. The thickness of the carbon nanotube/polymer layer is about 600 nm. Nanocomposite membranes with an additional polydimethylsiloxane (PDMS) coating on top of the original carbon nanotubes/PSF system have also been prepared. This structure is shown in Figure 2d.

High-resolution transmission electron microcopy (HRTEM) images of the CNT cross-sections in a polymer matrix are shown in Figure 3a. These images have been used to estimate the area density of the carbon nanotubes, which is $\sim(7.0 \pm 1.75) \times 10^{10}$ nanotubes per $cm^2$. Similar to HRTEM images of the acid-treated CNTs sample in Figure 1b,c, HRTEM images of nanotubes in the polymer matrix reveal mostly

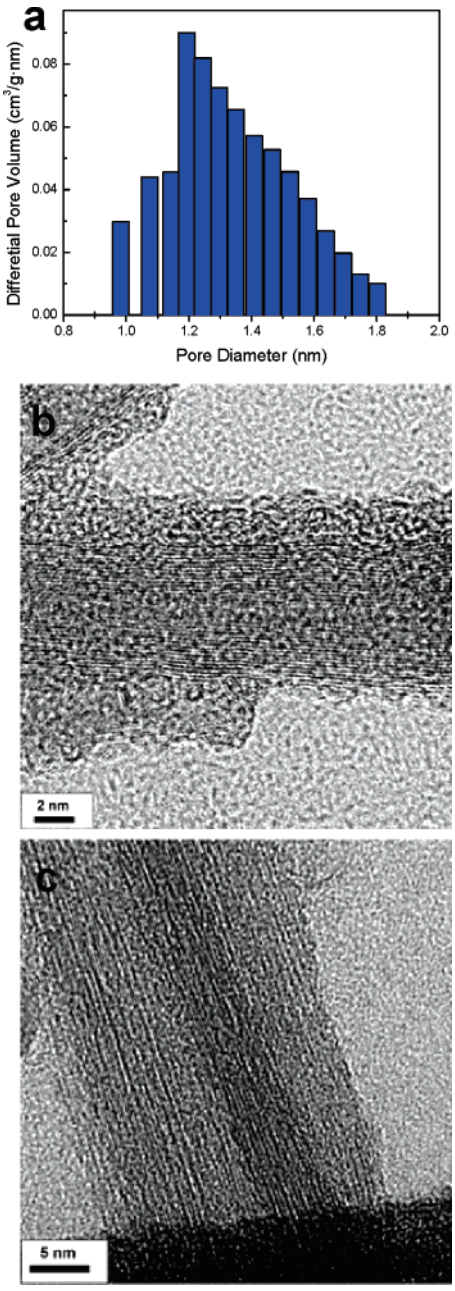


**Figure 1.** SWNT pore structure after acid treatment. (a) Differential pore volume plot of SWNT at 77 K using $N_2$. Pore diameter of the SWNT sample was calculated by the Horvath−Kawazoe (H−K) method. The H−K method used here was derived for cylindrical pores. The distribution in micropore diameter of the SWNT ranges from 0.95 to 1.8 nm, showing strong peak intensity at 1.2 nm. Therefore, the average pore diameter of the SWNT in this study is estimated to be 1.2 nm. (b) Zero-loss filtered (energy slit width of 10 eV) high-resolution TEM (HRTEM) image of multiwalled CNT that is transformed from SWNTs after acid treatment. (c) Zero-loss HRTEM image of several SWNT bundles. CNT samples for high-resolution TEM experiments were prepared by utilizing dimethylformamide (DMF) as solvent to disperse them on an ultrathin amorphous carbon support film.

two types of structures, namely encapsulated SWNT bundles and SWNTs with additional graphite sheets, as shown in Figure 3b. A single SWNT that has been transformed into a MWNT by encapsulation with additional graphite layers is shown in Figure 3c. It is likely that the increase in outer

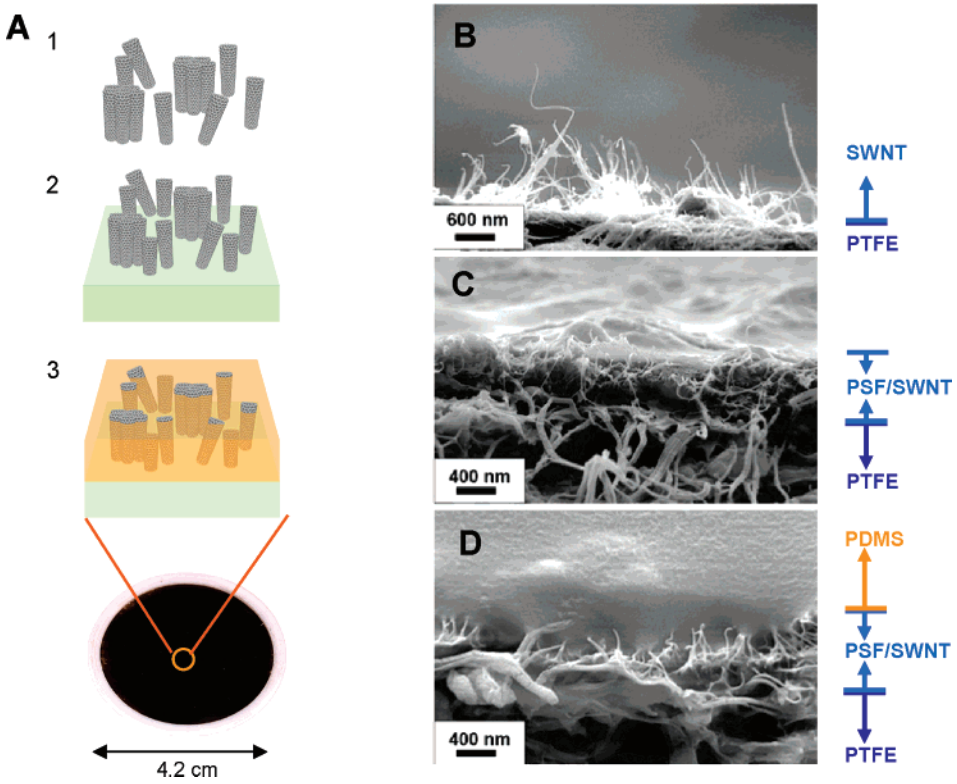


**Figure 2.** CNT nanocomposite membrane process. (a) Schematic membrane fabrication process. Step 1: the functionalized CNTs are dispersed in THF solution. Step 2: yhe CNTs/THF solution is filtered through 0.2 $\mu$m pore size hydrophobic polytetrafluoroethylene (PTFE) membrane filter. Step 3: the CNTs/PTFE is spin-coated with a dilute polymer solution. Some nanotube tips are embedded in polymer matrix. (b) Side-view SEM image of carbon nanotubes standing vertically on a membrane filter. (c) Side-view SEM image of aligned nanotube/PSF nanocomposite membrane after spin-coating. Polymer coating is so thin that some carbon nanotube tips are exposed on top of the surface. (d) Side-view SEM image of aligned nanotube/PSFPDMS composite membrane with a protective PDMS coating of 4 $\mu$m.

diameter of the transformed SWNT also aids in the vertical orientation of the carbon nanotube during the filtration process.

The quality of the CNT/PSF composite membrane has been tested by measuring its permeation to helium. In general, the transport of pure gases through a porous membrane can be described by one of three mechanisms: viscous flow, Knudsen diffusion, and surface flow.[21] Knudsen diffusion occurs when the mean free path of the gas molecules ($\lambda$) is larger than the pore radius ($r$) of the membrane, and there are more collisions with the pore walls than between gas molecules. When $r/\lambda$ becomes much larger than 1 ($r \gg \lambda$), as would be the case for gas transport in pinholes and other structural defects, viscous flow dominates the gas transport mechanism. Therefore, high-quality membranes can be characterized by the absence of viscous flow and more by Knudsen-like diffusion. For porous membranes that are governed by Knudsen diffusion, a plot of permeability versus average pressure should give a horizontal line because gas transport in a Knudsen regime is independent of the feed pressure. Alternatively, the permeation should increase with increasing pressure across the membrane when viscous flow takes place. As shown in Figure 4a, the helium permeance through the CNT membranes is independent of the pressure drop across the membrane. This is evidence that there is no viscous flow through any large pinholes and that the prepared SWNT membrane is defect free.

When Knudsen diffusion occurs, membrane permeance is inversely proportional to the square root of the molecular weight of the permeating gas molecule. Figure 4b shows the effective gas permeability in the two oriented CNT/polymer nanocomposite membranes as a function of the square root of the reciprocal of the gas molecular weight, $M^{-1/2}$. The solid line represents the Knudsen flow model. While the permeabilities of all samples are approximately proportional to $M^{-1/2}$, the absolute permeability of the CNT/PSF membrane is significantly higher than that predicted by Knudsen diffusion. This indicates that the gas transport in this sample takes place primarily through the carbon nanotubes, with very little transport through the ultrathin polymer matrix. This gas flow enhancement above the Knudsen regime is consistent with the atomistic simulations discussed previously[10] and the previous experimental observations of Holt et al.[6] On the other hand, the permeabilities of the sample having an additional polymer coating, CNT/PSF/PDMS, are lower than those predicted by the Knudsen diffusion model. This decrease in permeability is proportional to the transport resistance offered by the additional polymer layer. Some of the deviation of $CO_2$ permeance from the Knudsen scaling in this membrane is due the higher sorption of $CO_2$ in the PDMS layer relative to the other gases.[22]

Figure 4c shows the single-gas selectivities for various gas/helium pairs of the two CNTs membranes as a function of the gas molecular weight. With the exception of $CO_2$, the

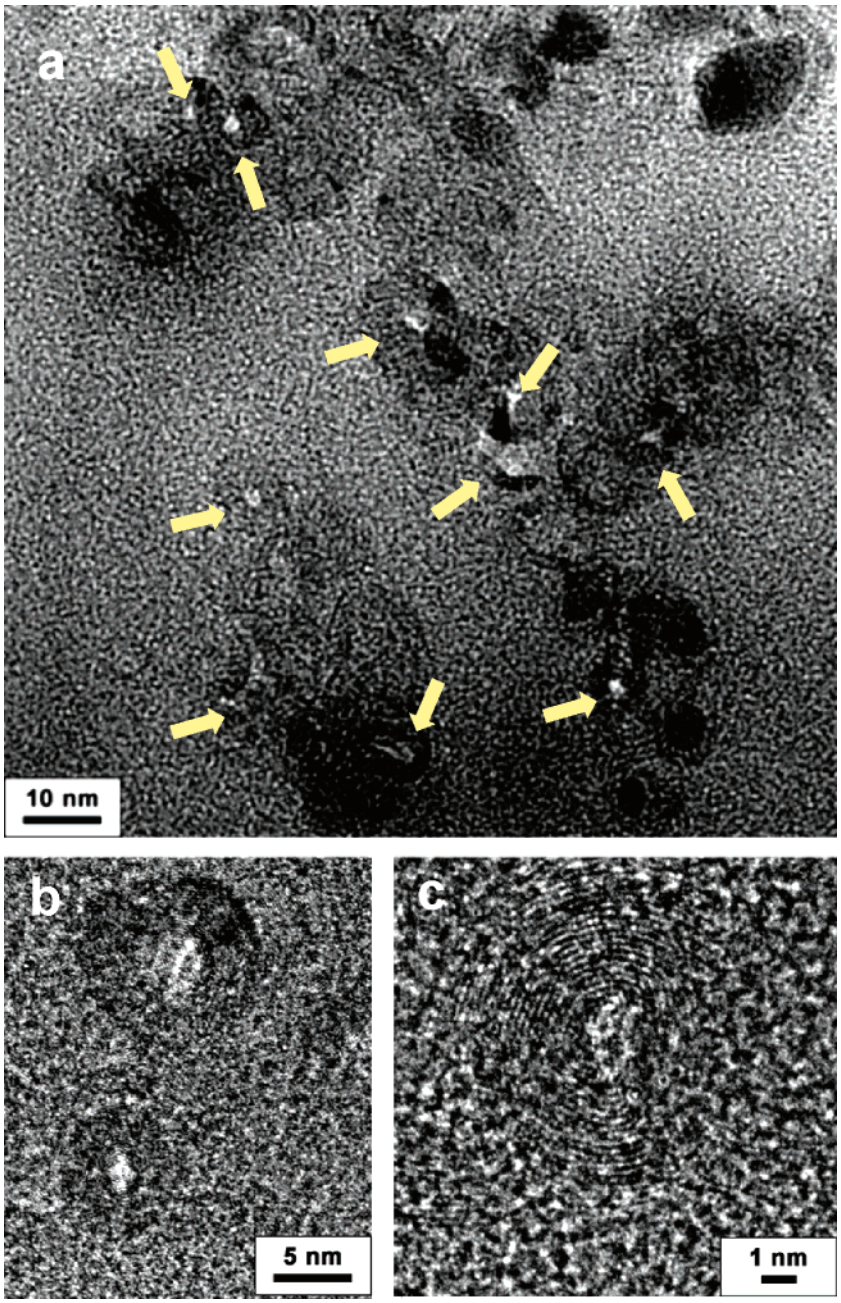


**Figure 3.** HRTEM images in plan-view orientation of CNTs in a polymer matrix. The TEM specimen has been coated with a thin amorphous carbon film prior to the TEM experiment to prevent specimen charging. In (a), bright-white spots (indicated by arrows) represent open nanotube pores. (b and c) HRTEM images at higher magnification reveal the structure of these pores. In (b), an encapsulated SWNT bundle is shown in the upper part of the image, and an encapsulated individual SWNT is in the lower part of the image. This SWNT bundle has an inner diameter of 4 nm. (c) The individual SWNT with an inner diameter of ~1.5 nm is clearly encapsulated by additional graphite layers. The area density of SWNTs was measured to be $\sim(7.0 \pm 1.75) \times 10^{10}/\text{cm}^2$ from several HRTEM images.

selectivity exhibits the inverse square root of the molecular mass dependence predicted by the Knudsen diffusion model. Again, the higher-than-Knudsen selectivity of the $CO_2$/He gas pair in the CNT/PSF/PDMS membrane can be attributed to the high solubility of $CO_2$ in the PDMS layer.

The permeation of gas mixtures through porous membranes provides a more stringent test of the transport mechanism than single-gas experiments. If transport occurs via Knudsen diffusion, the selectivity observed from single-gas experiments and mixed-gas experiments would be identical. Figure 4d compares the selectivities of one of our CNT/PSF membranes for $CO_2/CH_4$ as single gases and for permeation of a 50:50 feed mixture. The mixed-gas selectivity is significantly different from the single-gas experiments, so this example deviates strongly from Knudsen behavior.

To further probe these mixture results, we have adapted previous atomistic simulations to examine transport of $CO_2/CH_4$ mixtures in single CNTs. These simulations describe defect-free (10,10) nanotubes (diameter 1.36 nm) of infinite extent.[10,11,23] By separately computing adsorption isotherms and loading-dependent transport diffusion coefficients, predictions can be made for permeation through CNT mem-

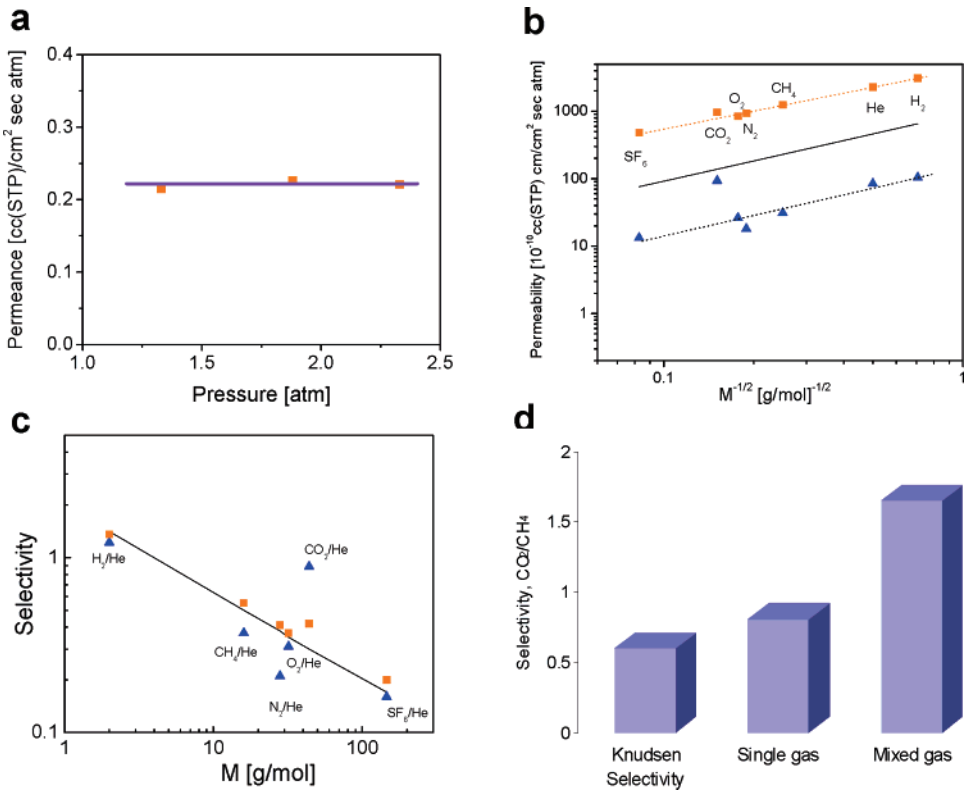


**Figure 4.** Gas transport properties of CNT nanocomposite membrane. Gas transport properties of CNT/PSF/PDMS membrane (blue triangle), CNTs/PSF membrane (orange square), and Knudsen diffusion model (solid line). (a) Effect of the pressure drop on the permeance of helium through CNTs/PSF membrane. (b) Single-gas permeability as a function of the inverse square root of the molecular weight of the penetrant. (c) Single-gas selectivity with respect to helium calculated from single-gas permeability data. (d) Mixed-gas selectivity ($CO_2$/$CH_4$) of CNTs/PSF membrane. The composition of gas mixture was $CO_2$:$CH_4$ = 50:50. The feed pressure was 50 psi, and the pressure differential across membrane was maintained by drawing a vacuum on the permeate side. Operating temperature was maintained at 308 K.

branes.[11,13] Binary adsorption isotherms were predicted by applying ideal adsorbed solution theory (IAST) to the single-component isotherms from atomistic simulations. IAST is known to be accurate for these systems.[24] Binary transport diffusivities were predicted from the single-component diffusivities from atomistic simulations by using the methods of Skoulidas, Sholl, and Krishna (SSK).[25] This method has been shown to be accurate for a range of similar systems via detailed atomistic simulations of mixture diffusion.[25] We have explored a broad range of feed pressures, compositions, and transmembrane pressure drops with these calculations; they predict $CO_2$/$CH_4$ selectivities varying between ~2 and 10, depending on operating conditions. For conditions similar to our experiments (50:50 feed composition, 50 psi feed, 0.7 psi permeate), our calculations predict a $CO_2$/$CH_4$ selectivity of 5.1. We also performed experiments with a $CO_2$ mole fraction of 0.2, 0.5, and 0.8 in the membrane feed using three different nanocomposite membranes. The averaged experimental results along with the theoretical predictions are shown in Figure 5. The error bars on the experimental data reflect the variability in the sample preparation method. Our theoretical predictions give mixture selectivities that are considerably larger than our experimental observations. The predictions do, however, reproduce the non-Knudsen selectivity of the experiments. Briefly, the diffusion of isolated molecules in our simulations differs from

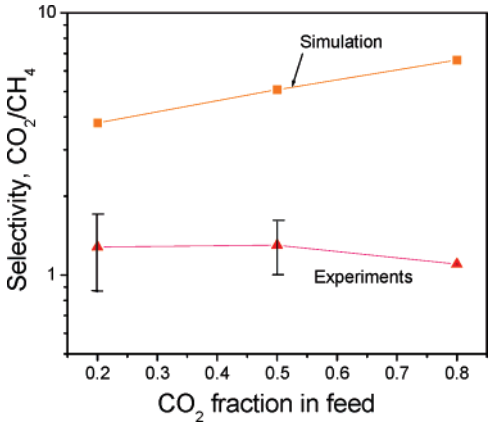


**Figure 5.** Mixed-gas selectivity ($CO_2$/$CH_4$) of CNTs/PSF membrane at different $CO_2$ feed composition. Both experimental and simulation conditions assumed a feed pressure of 50 psi and a temperature of 308 K. The pressure differential across membrane was maintained by drawing a vacuum on the permeate side.

Knudsen diffusion because both species adsorb on the walls of CNTs and individual collisions between molecules and the CNT walls do not completely thermalize the molecular momenta.[9,11] In the mixture, the more strongly adsorbing $CO_2$ partially excludes $CH_4$ from CNTs and the slower diffusing $CO_2$ molecules reduce the mobility of adsorbed $CH_4$. Both

of these effects increase the selectivity of the membrane relative to the result of single-gas operation.[26]

There are three important caveats in comparing these atomistic calculations with our experimental data. First, the calculations are based solely on (10,10) CNTs. The importance of adsorption in larger CNTs is likely to be lower than in the relatively small pores of (10,10) CNTs. Diffusion coefficients for $CO_2$ from atomistic simulations are known to decrease as pore sizes increase,[23] but insufficient data is currently available to accurately predict the properties of permeating mixtures in these CNTs. Second, our calculations assumed that membrane transport is dominated by intrapore diffusion. In short enough nanotubes, however, transport resistances associated with entering and leaving pores may also contribute. Estimates of these resistances for (20, 0) nanotubes for $CH_4$ permeation indicate that they may not be negligible for CNTs of the lengths observed in our experiment ($<1\ \mu$m).[27] Similar estimates are not available for $CO_2$ or for permeating mixtures, but related work on zeolites suggests that surface resistances should in general be more important for more strongly adsorbing molecules.[28] This would suggest that $CO_2$ transport through CNTs would be more strongly affected by pore entrance/exit effects than $CH_4$, potentially reducing the overall membrane selectivity. Third, our calculations assume the pore entrances of the CNTs are not functionalized. As stated above, the CNTs in our fabricated membranes are likely to be functionalized by zwitterions around pore mouths. Although we do not know the density of these functionalizing groups, it is likely that they contribute to the overall performance of the membrane. In other studies, functional groups at the end of MWNTs have been utilized to investigate a "gatekeeper" mechanism for controlling the selectivity of chemical transport through the CNT membranes.[29] Amine functional groups have widely been used to modify sorbents and catalysts to increase $CO_2$ selectivity by carbamate formation in the absence of water.[30] It is therefore likely that the selectivity for $CO_2$-containing mixtures we observe in our membranes is due in part to the transport effects inside CNTs that were probed by our atomistic calculations and in part due to pore entrance/exit effects involving functionalization of the pore mouths.

In summary, the filtration method presented here facilitates the orientation of carbon nanotubes on porous supports and can be easily adapted to large-scale membrane formation. The resulting nanocomposite membranes have the same fast gas transport properties as those observed in carbon nanotube membranes grown by chemical vapor deposition. Our results include the first characterization of gas mixture transport through CNT-based membranes. These results indicate that it is possible to achieve rapid transport through CNT membranes that deviates from Knudsen selectivities.

**Acknowledgment.** This research was supported by National Science Foundation with grant CTS-04003692. We are grateful to Dr. Yushan Yan for helpful discussions. We also thank Steve McCartney for his help with the FESEM images.

**Supporting Information Available:** Extended description of the experimental setup and calculation of the equivalent Knudsen flow are provided. This material is available free of charge via the Internet at http://pubs.acs.org.

## References

(1) Kong, J.; Franklin, N. R.; Zhou, C.; Chapline, M. G.; Peng, S.; Cho, K.; Dai, H. *Science* **2000**, *28*, 622−625.
(2) Collins, P. G.; Bradley, K.; Ishigami, M.; Zettl, A. *Science* **2000**, *287*, 1801−1804.
(3) Calvert, P. *Nature* **1999**, *399*, 210.
(4) Planeix, J. M.; Coustel, N.; Coq, B.; Brotons, V.; Kumbhar, P. S.; Dutartre, R.; Geneste, P.; Bernier, P.; Ajayan, P. M. *J. Am. Chem. Soc.* **1999**, *116*, 7935−7936.
(5) Hinds, B. J.; Chopra, N.; Rantell, T.; Andrews, R.; Gavalas, V.; Bachas, L. G. *Science* **2003**, *303*, 62−65.
(6) Holt, J. K.; Park, H. G.; Wang, Y.; Stadermann, M.; Artyukhin, A. B.; Grigoropoulos, C. P.; Noy, A.; Bakajin, O. *Science* **2006**, *312*, 1034−1037.
(7) Qin, L.-C.; Zhao, X.; Hirahara, K.; Miyamoto, Y.; Ando, Y.; Iijima, S. *Nature* **2000**, *408*, 50.
(8) Wang, N.; Tang, Z. K.; Li, G. D.; Chen, J. S. *Nature* **2000**, *408*, 50.
(9) Ackerman, D. M.; Skoulidas, A. I.; Sholl, D. S.; Johnson, J. K. *Mol. Simul.* **2003**, *29*, 677−684.
(10) Skoulidas, A. I.; Ackerman, D. M.; Johnson, J. K.; Sholl, D. S. *Phys. Rev. Lett.* **2002**, *89*, 185901-4.
(11) Chen, H.; Johnson, J. K.; Sholl, D. S. *J. Phys. Chem. B* **2006**, *110*, 1971−1975.
(12) Chen, H.; Sholl, D. S. *J. Am. Chem. Soc.* **2004**, *126*, 7778−7779.
(13) Chen, H.; Sholl, D. S. *J. Membr. Sci.* **2006**, *269*, 152−160.
(14) Majumder, M.; Chopra, N.; Andrews, R.; Hinds, B. J. *Nature* **2005**, *438*, 44.
(15) der Heer, W. A.; Bacsa, W. S.; Chatelain, A.; Gerfin, T.; Humphrey-Baker, R.; Forro, L.; Ugarte, D. *Science* **1995**, *268*, 845−847.
(16) Li, W.; Wang, X.; Chen, Z.; Waje, M.; Yan, Y. *Langmuir* **2005**, *21*, 9386−9389.
(17) Fan, Z. H.; Advani, S. G. *Polymer* **2005**, *46*, 5232−5240.
(18) Hoagland, D. A. *Macromolecules* **1990**, *23*, 2781−2789.
(19) Liu, J.; Rinzler, A. G.; Dai, H.; Hafner, J. H.; Bradley, R. K.; Boul, P. J.; Lu, A.; Iverson, T.; Shelimov, K.; Huffman, C. B.; Rodriguez-Macias, F.; Shon, Y.; Lee, T. R.; Colbert, D. T.; Smalley, R. E. *Science* **1998**, *280*, 1253−1256.
(20) An, K. H.; Jeon, K. K.; Moon, J.-M.; Eum, S. J.; Yang, C. W.; Park, G.-S.; Park, C. Y.; Lee, Y. H. *Synth. Met.* **2004**, *140*, 1−8.
(21) Uhlhorn, R. J. R.; Keizer, K.; Burggraff, A. J. *J. Membr. Sci.* **1989**, *46*, 225−241.
(22) Merkel, T. C.; Bondar, V. I.; Nagai, K.; Freeman, B. D.; Pinnau, I. *J. Polym. Sci., Part B: Polym. Phys.* **2000**, *38*, 415−434.
(23) Skoulidas, A. I.; Sholl, D. S.; Johnson, J. K. *J. Chem. Phys.* **2006**, *124*, 054708.
(24) Chen, H.; Sholl, D. S. *Langmuir* **2007**, *23*, 6431−6437.
(25) Skoulidas, A. I.; Sholl, D. S.; Krishna, R. *Langmuir* **2003**, *19*, 7977−7988.
(26) Sholl, D. S. *Acc. Chem. Res.* **2006**, *39*, 403−411.
(27) Newsome, D. A.; Sholl, D. S. *Nano Lett.* **2006**, *6*, 2150−2153.
(28) Newsome, D. A.; Sholl, D. S. Atomically-detailed Simulations of Surface Resistances to Transport of $CH_4$, $CF_4$ and $C_2H_6$ through Silicalite Membranes. *Microporous Mesoporous Mater.* **2007**, http://dx.doi.org/10.1016/j.micromeso.2007.03.016.
(29) Majumder, M.; Chopra, N.; Hinds, B. J. *J. Am. Chem. Soc.* **2005**, *127*, 9062−9070.
(30) Satyapal, S.; Filburn, T.; Trela, J.; Strange, J. *Energy Fuels* **2001**, *15*, 250−255.

NL071414U